29th Congress of the International Council
of the Aeronautical Sciences
St. Petersburg, Russia; September 7–12, 2014

PROBLEM OF LOW CYCLE FATIGUE OF TURBOMACHINES

Joury Temis*, Khakim Azmetov* and Alexander Fakeev*
*Department of Mathematical Simulation, Central Institute of Aviation Motors

Keywords: *thermomechanical fatigue, cyclic stress-strain loop*

Abstract

Model of cyclic stress-strain curve and corresponded damage model for simulation of nonisothermal cyclic loading and estimation of turbomachinery component life time are developed. Change of Bauschinger's effect, Young's modulus and parameters of hardening as functions of accumulative plastic strain are described by the cyclic model of material. Model of damage is based on reaching value of accumulative plastic strain to ultimate state at cyclic loading. Simulation of nonisothermal plasticity of turbomachinery components based on Finite Element Method [FEM] code which uses the theory of strain plasticity for calculation that was generalized to cyclic nonisothermal loading. Results of calculation of turbine engine components such as discs, high-loaded concentrators of blade locks and turbine blades under cyclic loading are presented.

1 Introduction

Turbomachinery components work under nonisothermal and transient loading which generates alternating plastic strain under strain cycling in stress concentrator. Therefore problem of mathematical simulation of stress-strain state is actual to describe influence of plasticity and creep under nonisothermal cyclic loading. Particularly this problem is actual on the design stage of Gas Turbine Engine [GTE] parts with the stress concentrators (discs with holes, turbine blades and etc.) for estimating of low cycle fatigue [LCF]. These stress concentrators are local and change stresses and strains from the nominal values in the some local regions of components. Therefore in the most cases stresses and strains in these regions practically have not influence on the common stress-strain state of the component. Common stress-strain state can be described by calculating of kinetics of stresses and strains in the structure. It is possible on the base of the technology of multidisciplinary simulation that allows creating virtual model of component or engine [1-3]. This virtual model evaluates the kinetics of thermal state, pressures, nominal displacements, strain and stresses in the components of structures by the simultaneously calculating gas flow in the cavities of the engine, transient thermal conductivity and deformable solid mechanics. Results of that analysis determine temperatures and boundary conditions (displacements and stresses) for the improvement of the selected region around the concentrator.

Transition to research of region of concentrator requires more accuracy analysis of elastoplastic state. In that case it is necessary to take into account features of nonisothermal cyclic loading. Cyclic stress-strain curve presents a conception about these features. This paper dedicates to describe of models simulating of kinetics of stress-strain state and life prediction of low cycle fatigue of concentrator region. Models of plasticity using in the paper are based on approximation cyclic stress-strain curve by three parameters describing of Bauschinger's effect, scale of transformation of nonlinear part of stress-strain curve and Young's modulus and depending on total accumulative plastic strain [4]. Nonisothermal loading is considered by the conception of thermomechanical surface [5] generalizing on nonisothermal cyclic loading.

2 Theory

2.1 Model of nonisothermal cyclic stress-strain curve

Three parametric model [6, 7] using for simulation of elastoplastic stress-strain response under isothermal cyclic loading is generalized to case of nonisothermal conditions. This makes possible to describe dependence of Bauschinger's effect, nonlinear part of stress-strain curve and Young's modulus versus total accumulative plastic strain under nonisothermal cyclic loading. Such approach at fixed temperatures was confirmed for description cyclic stress-strain curve several structural materials [6, 7].

The thermomechanical surface under cyclic or complex loading is considered. Part of this thermomechanical surface locating between isothermal cyclic stress-strain curves at temperatures T_1, T_2 and at current value of accumulative plastic strain $\chi = \int |d\varepsilon^p|$ is described by relations:

$$\sigma^* = F(\varepsilon_p^*, T),$$
$$F = (1-\lambda)f_1 + \lambda f_2,$$
$$\lambda = \frac{T - T_1}{T_2 - T_1} \quad (1)$$

$$f_i = \begin{cases} E(T_i) \cdot d(\chi, T_i) \cdot \varepsilon^*, & \varepsilon^* \leq \varepsilon_s^* \\ \\ E(T_i) \cdot d(\chi, T_i) \cdot \varepsilon_s^* + \\ + d(\chi, T_i) \cdot b(\chi, T_i) \cdot \\ \cdot \left[f\left(\varepsilon_s + \frac{\varepsilon^* - \varepsilon_s^*}{b(\chi, T_i)}, T_i \right) - \sigma_s(T_i) \right], & \varepsilon^* > \varepsilon_s^* \end{cases} \quad (2)$$

$$i = 1, 2; \quad \sigma_s^*(T_i) = a(\chi, T_i) \cdot \sigma_s;$$
$$\varepsilon_s^*(T_i) = a(\chi, T_i) / d(\chi, T_i) \cdot \varepsilon_s$$

where σ^* and ε^* are stress and strain in local coordinate system respectively (Fig. 1a); $a(\chi, T)$ is a size of elastic zone of loading surface; $b(\chi, T)$ is a transformation coefficient of nonlinear part of initial stress-strain curve; $d(\chi, T)$ is a coefficient of variation of Young's modulus; ε_s and σ_s are the initial yield stress and strain; ε_p is a plastic strain; E is a initial Young's modulus; $f(\varepsilon, T)$ is a stress-strain curve at the first halfcycle; f_i is a cyclic stress-strain curve at temperature T_i [6, 7].

It should be noted that parameters $a(\chi, T_i)$, $b(\chi, T_i)$ and $d(\chi, T_i)$ depend on accumulative plastic strain χ and characterize cyclic stress-strain curve at temperature T_i.
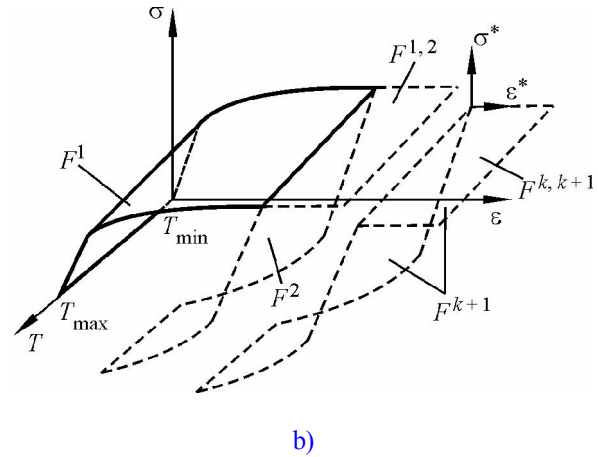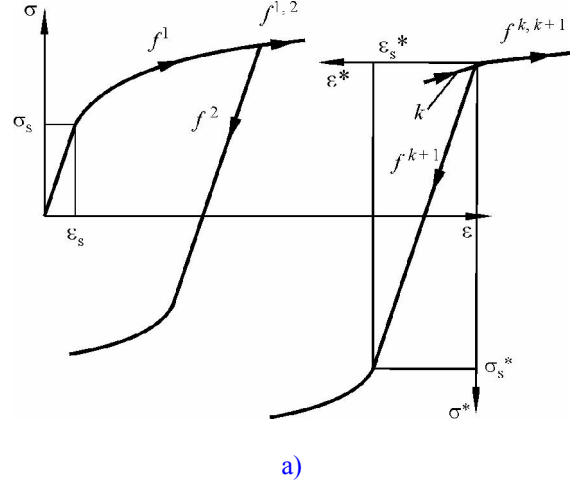

a)

b)

Fig. 1. Model of thermomechanical surface: a) - stress-strain curve for isothermal cyclic loading; b) - part of thermomechanical surface at various halfcycles

For simulation of nonisothermal cyclic loading it is necessary to calculate isothermal stress-strain curve f_i^{k+1} for temperature T_i on the each $k+1$ halfcycle (Fig. 1a). Also it is necessary to take account of plastic strain χ^k accumulated in previous halfcycles. Then thermomechanical surface F_i^{k+1} is calculated for the $k+1$ halfcycle (Fig. 1b). Nonisothermal cyclic stress-strain curve on the $k+1$ halfcycle is located on this surface in stress-strain-temperature coordinates. Determining parameters of this surface is occurred with taking into account of direction of loading.

Material parameters $a(\chi,T)$, $b(\chi,T)$ and $d(\chi,T)$ using for variation of cyclic curves under isothermal loading are depended as function on accumulative plastic strain. For various temperatures these parameters are determined from experimental isothermal stress-strain curves under hard or soft loading. After determining $\chi(n,T)$, $a(n,T)$, $b(n,T)$ and $d(n,T)$ for each temperature it may be possible to determine required relations $a(\chi,T)$, $b(\chi,T)$ and $d(\chi,T)$ for required temperature and accumulated plastic strain range.

2.2 Model verification

Based on the equations (1) and (2) a program of experimental data processing and simulation of specimen test under nonisothermal cyclic loading was developed. Verification of this program under isothermal and nonisothermal loading was performed in paper [8].

Experimental results of nickel based superalloy under isothermal and nonisothermal cyclic loading were presented in [9]. Frequency of isothermal and nonisothermal loading was 0.0025 Hz (400 seconds per cycle). Influence of creep strain was neglected. Temperature of all experiments was in range from 571°C to 823°C. Type of loading cycle was hard. Stress-strain curves and material parameters were defined from isothermal tests. Material parameters a and b of the alloy at temperatures 571°C, 700°C, 823°C is shown on Fig. 2.

Simulation of in-phase and out-phase tests are carried out. The 67th and 68th halfcycles for all types of loading is considered as stable hysteresis loop. In both cases of the simulation loops for 1-3, 10-11, 30-31 and 67-68 halfcycles are shown on Fig. 3.
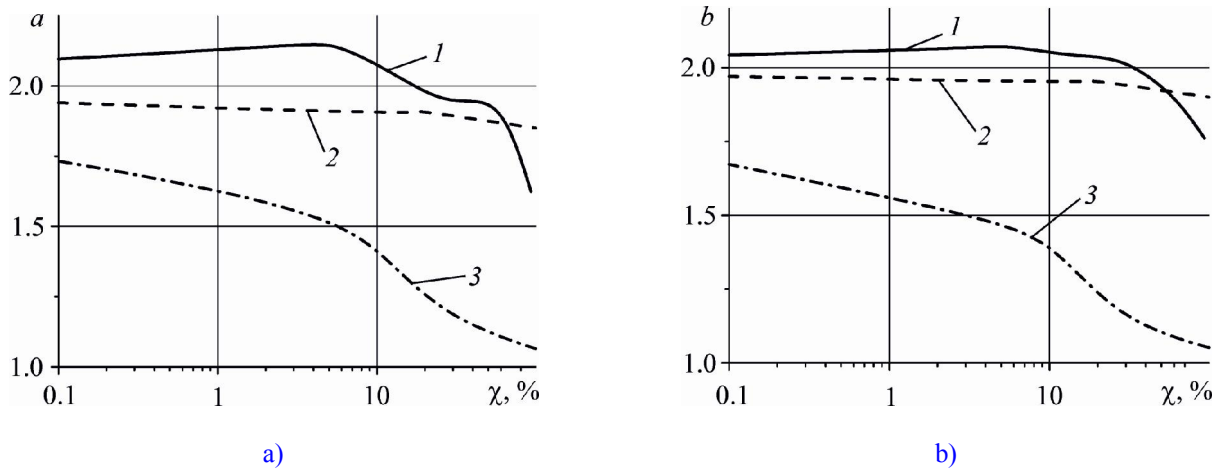

a)

b)

Fig. 2. Material parameters at different temperatures: a) parameter a; b) parameter b (1 - 571°C, 2 - 700°C, 3 – 823°C)
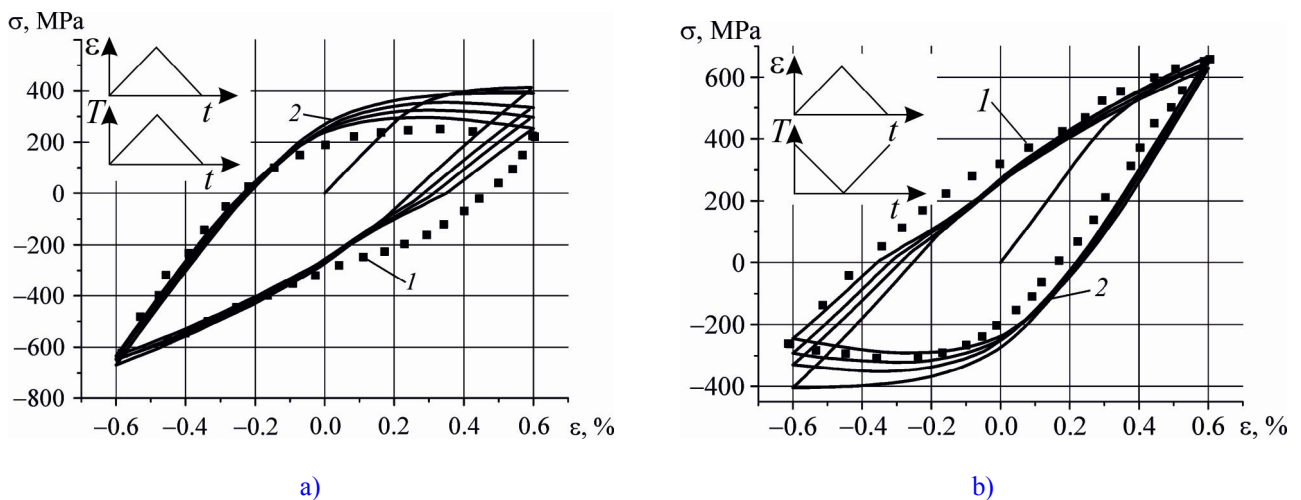

a)

b)

Fig. 3. Hysteresis loops under nonisothermal loading: a) in-phase test; b) out-phase test (1 - experiment, 2 - simulation)

Comparison of experimental data of stable hysteresis loop and results of simulation of in-phase test is shown on Fig. 3a. Strain amplitude was equal 0.6%. Temperature was equal 823°C at maximum of tension and temperature was equal 571°C at maximum of compression.

Simulation and experimental results of stable hysteresis loop of out-phase test are shown on Fig. 3b. Parameters of out-phase test were equivalent to ones of in-phase test.
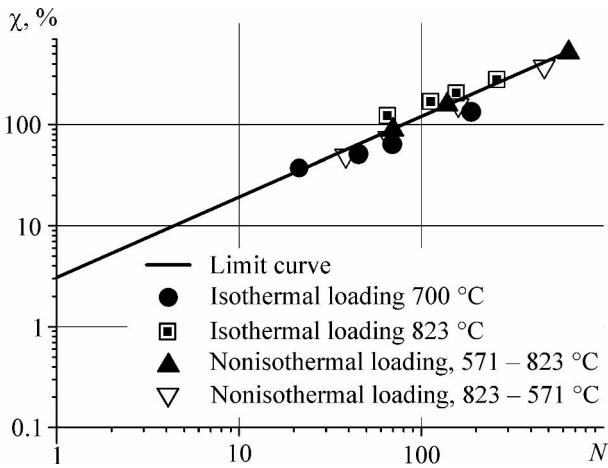
2.3 Damage model

In papers [4, 6, 7] based on experimental results it was determined that at room temperature the number of halfcycles to failure n_f for several structural materials under various loading programs (soft loading, hard loading, random loading) depends on ultimate value of accumulated plastic strain χ_{max} by next relation:

$$n_f = (\chi_{max} / \delta)^{\gamma} \qquad (3)$$

where δ and γ is material constants.

LCF isothermal experimental data at temperatures 700°C and 823°C [9] allow by least-squares method to calculate material parameters δ and γ of the damage model. Accumulative plastic strain as function of the number of cycles to failure was calculated by the model (1-2). For comparison on Fig. 4a experimental results of LCF are shown by points and result of the damage model (3) is shown by limit curve that is calculated by

parameters δ and γ.

Similarly based on LCF experimental data of IN738LC alloy [10] in temperature range 400°C - 900°C applicability of the damage model was verified. Based on isothermal data at 400°C and 900°C the parameters of the LCF model were calculated by least-squares method. Experimental results of LCF are shown on Fig. 4b by points. Limit curve on Fig. 4b is calculated by parameters δ and γ that were defined from experimental data.
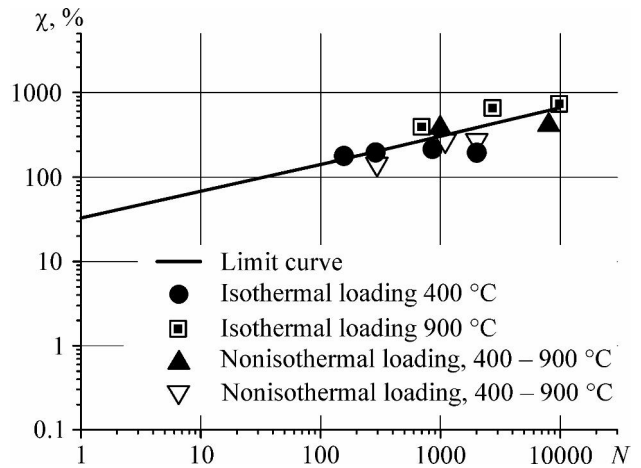
3 Finite element analysis

Consider cyclic deformation when load vector $\{F\}$ is applied to component by the following program

$$0 \rightarrow \{F_{max}\} \rightarrow \{F_{min}\} \rightarrow \{F_{max}\} \rightarrow ... \qquad (4)$$

If strain and stress vectors in body points $\{\varepsilon\}_k$ and $\{\sigma\}_k$ correspond to end of the kth halfcycle of loading and ones $\{\varepsilon\}_{k+1}$ and $\{\sigma\}_{k+1}$ correspond to end of the $(k + 1)^{th}$ halfcycle then for each halfcycle a variational relationship is carried out

$$\int_{\Omega} \{\sigma\}_q^T \{\delta\varepsilon\} d\Omega -$$
$$- \int_{\Omega} \{F_{\Omega}\}_q^T \{\delta u\} d\Omega - \int_{S} \{F_S\}_q \{\delta u\} dS = \qquad (5)$$
$$= \int_{\Omega} \{R_{\Omega}\}_q^T \{\delta u\} d\Omega - \int_{S} \{R_S\}_q \{\delta u\} dS$$

a)

b)

Fig. 4. Relation between cumulated plastic strain to failure χ_{max} and number of halfcycles to failure: a) nickel-base superalloy, b) IN738LC alloy

where $q = k, k + 1$ – the halfcycle number; $\{F_\Omega\}$, $\{R_\Omega\}$, $\{F_S\}$, $\{R_S\}$ – vectors of volume loads and misalignment and surface loads and misalignment respectively.

To suppose that $\{R_\Omega\}$, $\{R_S\}$ are equal zero on the $(k + 1)^{\text{th}}$ halfcycle and subtract from relation (4) at $q = k + 1$ similar one at $q = k$ it is obtained that a problem of stress-strain condition simulation by change of loading halfcycle is came to solution a next problem

$$\int_\Omega \{\Delta\sigma\}_{k+1}^T \{\delta\varepsilon\}d\Omega -$$

$$-\int_\Omega \{\Delta F_\Omega\}_{k+1}^T \{\delta u\}d\Omega - \int_S \{\Delta F_S\}_{k+1} \{\delta u\}dS = \quad (6)$$

$$= \int_\Omega \{R_\Omega\}_k^T \{\delta u\}d\Omega - \int_S \{R_S\}_k \{\delta u\}dS$$

If specify a relation form $\Delta\sigma(\Delta\varepsilon)$ the equation (6) by well-known method will be came to finite element problem

$$[K]_{k+1} \cdot \{\Delta U_{k+1}\} = \{\Delta F_{k+1}\} + \beta\{F_0\} \quad (7)$$

where $[K]_{k+1}$ – stiffness matrix of the $(k + 1)^{\text{th}}$ halfcycle defining by step-by-step approach; $\{\Delta U_{k+1}\}$ and $\{\Delta F_{k+1}\}$ – vectors of increments of displacement and loading at halfcycle, correspondingly; β – correcting multiply; $\{F_0\}$ – correcting vector.

In that case for displacement vector at the $(k + 1)^{\text{th}}$ halfcycle it is rightly

$$\{U_{k+1}\} = \{U_k\} + \{\Delta U_{k+1}\}, \quad (8)$$

while strain and stress in a calculated point are related by similar relations

$$\begin{aligned}\{\varepsilon_{k+1}\} &= \{\varepsilon_k\} + \{\Delta\varepsilon_{k+1}\}; \\ \{\sigma_{k+1}\} &= \{\sigma_k\} + \{\Delta\sigma_{k+1}\}. \end{aligned} \quad (9)$$

The equations (6)–(8) shows self–corrected algorithm for the problem solution. It can be considered to various models of plasticity depending on features of cyclic loading.

For the most components of turbomachine processes of force and temperature variation are synchronous. In this case it can be assumed that variations of stresses and strains are proportional.

These conditions are described by strain plasticity theory which was generalized on cyclic loading [11]. Plastic strains appear in the local region by the influence of elastic displacements of the all structure on the boundary which validates this assumption. This type of loading is similar to "hard" one. In this case it can be possible to consider large values of increments of loads, temperatures, stresses, strains and displacements and each step is considered as one half-cycle.

4 Calculation results

4.1 Overspeed test

The simulation of the overspeed test of the discs is considered (Fig. 5). Strain plasticity theory which was generalized on cyclic loading is applied in the simulation because experiments were carried out at constant temperature.
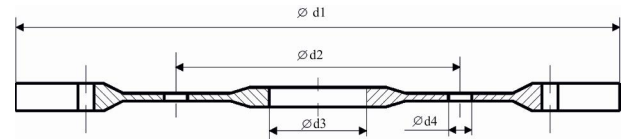

Fig. 5. Overspeed test disc scheme

Generalized planar stressed state was simulated in the discs. All computations were carried out by FEM analysis. For the improving of accuracy of analysis and numerical stability kinematic boundary conditions was defined in integral form. In the simulation of the overspeed tests a rotation frequency increased up to fracture initiation which was determined by non-stop node displacement increasing after fracture some finite elements. On each halfcycle damage failure level $D = \chi(n) / \chi_{\max}(n)$ is determining in the process of analysis. If damage failure level in an element verges towards unity the element is excluded from analysis by technology of "died" elements [11].

On Fig. 6 relations of radial displacements of points of disc hub and rim versus disc rotation frequency are shown. Displacements sharply increase at the critical revolution and fracture initiation of the disc is beginning.

On the Fig. 7 possible patterns of disc fracture with various numbers of holes are shown. The disc with six holes failed at crack propagation to the meridional direction

(Fig. 7a). The disc with ten holes begins to fail to the cylindrical direction then crack propagation continues to the radial direction (Fig. 7b). The disc with twelve holes failed at crack propagation to the cylindrical direction (Fig. 7c).
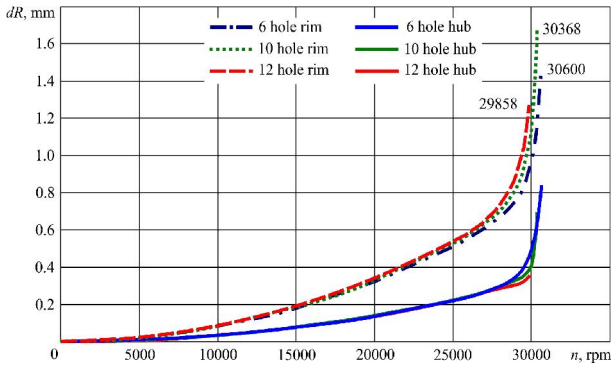

Fig. 6. Displacements of points of disk hub and rim at the radial direction versus rotation frequency
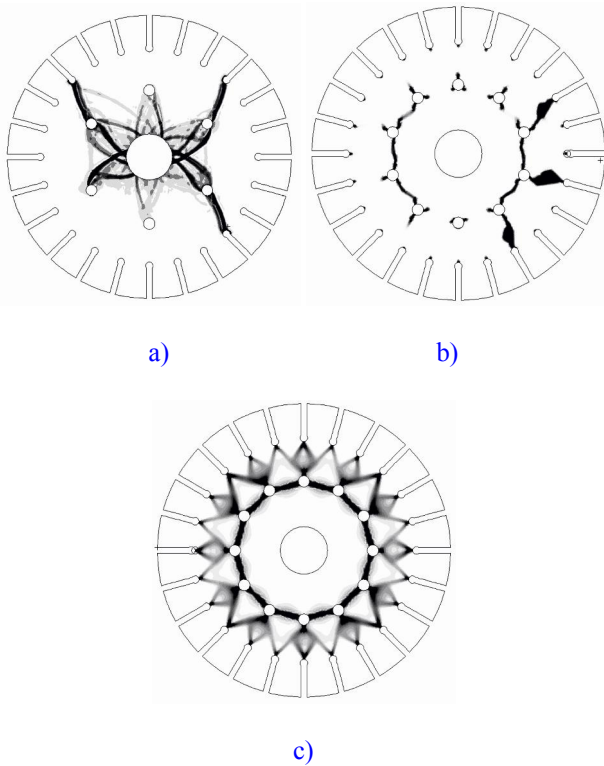

a)   b)

c)

Fig. 7. Overspeed test fracture pattern: a) 6 holes disc; b) 10 holes disc; c) 12 holes disc

Results of simulation of plasticity regions show that types of disc fracture correspond to model of limiting state which can be developed based on method of characteristics for rigid-plastic body.

Simulation of cyclic loading leads to the similar patterns of failure. However maximal

rotation frequency in the cycle is defined the values of number of cycles to failure. Therefore this model can be applied to the analysis of disc LCF.

4.2 Turbine disc lock

The turbine disc lock and equivalent notched specimen are considered (Fig. 8). All research was based on experimental results of low cycle fatigue of notched specimens under isothermal loading at the various temperatures that were carried out by T.K. Bragina in CIAM [12].
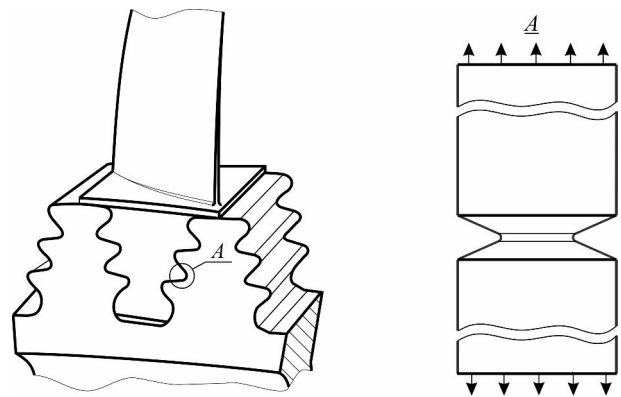

Fig. 8. Concentrators: a) turbine disc lock; b) equivalent specimen

Specimen material is nickel alloy AI698. Temperatures of experiments were 20°C, 400°C и 650°C. Type of loading was zero-to-compression stress cycle. Axisymmetric stress state was simulated in notched specimens.

Material parameters of cyclic model at the temperature 20°C and parameters of LCF model were performed in paper [11]. Material parameters of cyclic model at the temperature 600°C was calculated by the processing experimental data from paper [13]. Stress-stain state is shown on Fig. 9.

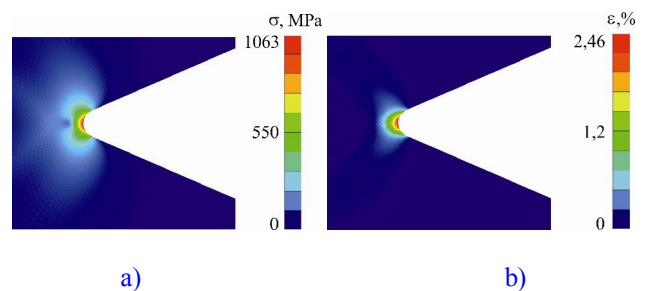
a)   b)

Fig. 9. Notched specimen at crack initiation under the stress amplitude 300 MPa and temperature 20°C: a) efficient stresses, b) efficient strains

Based on results of the cyclic loading LCF curves of the notched specimens under various stress amplitudes was calculated at the temperature 20°C (Fig. 10a) and 650°C (Fig. 10b). Simulation results are shown by lines and circles. Experimental results are shown by squares.
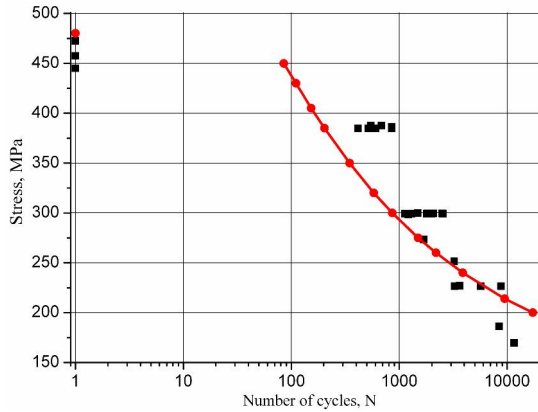

a)
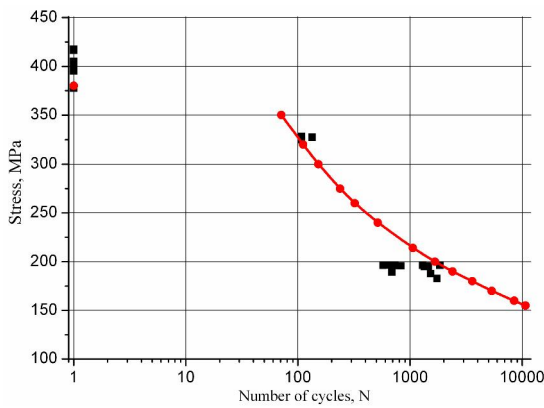
b)

Fig. 10. AI698 alloy LCF curve for notched specimens at different temperatures: a) 20°C, b) 650°C

4.3 LCF simulation of turbine blade

Numerical analysis of turbine blade is carried out. The turbine blade (Fig. 11a) works under nonisothermal cyclic loading (temperature range 20°C - 800°C in point A). Material of turbine blade is a nickel based superalloy.

There are holes for emission a cooling gas on the external surface in point A in the blade. Structural FEM analysis shows that maximum values of stress and plastic strain are located in the point A near the hole. Behavior of cyclic stress and cyclic strain near hole with strain
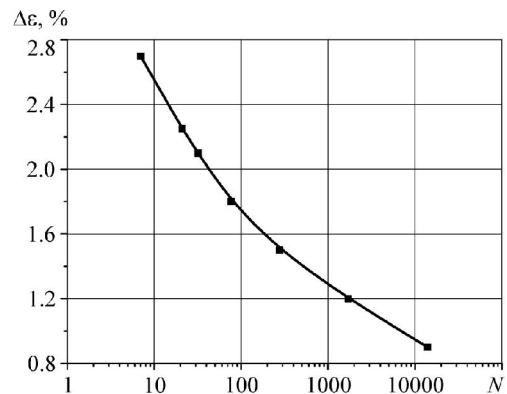
amplitude $\Delta\varepsilon = 1.5\%$ is shown on Fig. 11b. Modifying parameters of temperature and loading it is possible to estimate admissible strain near the hole and to calculate LCF curve (Fig. 11c).
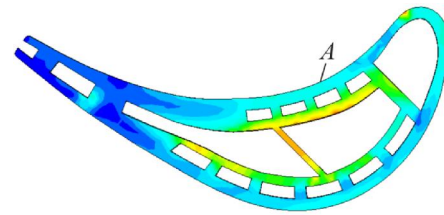
a)
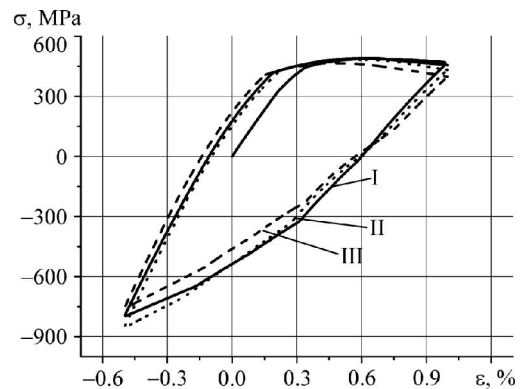
b)

c)

Fig. 11. Turbine blade FEM analysis: a) stress-strain state; b) cyclic stress-strain curve in the critical point (I – 1-2-3 halfcycles, II – 10-11 halfcycles, III – 50-51 halfcycles); c) turbine blade LCF curve

Process of crack growth and estimate of crack extension velocity are simulated by including "died" element model [11]. On the Fig. 12 the pattern 1 accords to the crack initiation in the hole for emission a cooling gas. The pattern 2 shows the middle of crack growth process and excepted "died" elements from

analysis which damage failure level was equal unity. The pattern 3 accords to moment when crack involves all volume between holes.
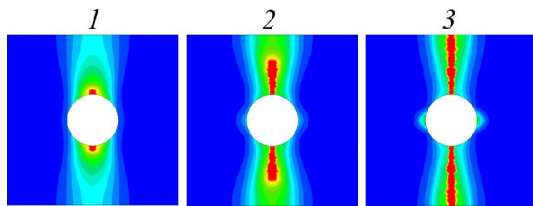

Fig. 12. Crack growth patterns in the critical point

6 Conclusion

Presented results indicate a probability of application of the nonisothermal cyclic stress-strain curve model generalizing the theory of strain deformation plasticity on cyclic nonisothermal loading and the damage model for calculation stress-strain state and life time prediction for high stressed structures of turbomachines under proportional loading.

For the complex loading an influence of forces and temperatures on the stress-strain state can be estimate if the time steps q are small and relation between stresses and strains is determined by theory of plastic flow that can be generalize on nonisothermal cyclic loading [14].

References

[1] Temis Y.M., Selivanov A.V. Thermomechanical model of engine. *Engineering Encyclopedia.* Vol. IV - 21, Book 3: *Aviation motors.* Editors: Skibin V.A., Temis Y.M., Sosunov V.A. Moscow: Mashinostroenie, 2010, pp 524-528. (In Russian).

[2] Temis Y.M., Selivanov A.V., Yurchenko G.G. Simulation of thermostressed state of HPC rotor with according secondary flow. *Herald of SGAU.* No. 6 (30), pp 148 – 156, 2011. (In Russian).

[3] Temis Y.M. Selivanov A.V., Yurchenko G.G. HPC Design Based on Multidisciplinary Numerical Simulation. *Proceedings of 10th European Conference on Turbomachinery: Fluid Dynamics and Thermodynamics ETC-2013*, Lappeenranta, Finland, pp 787- 796, 2013.

[4] Temis Y.M. Plasticity and creep of the GTE parts under cyclic loading. *Strength and Dynamic Problems in GTE.* Moscow, No. 4, pp 32-50, 1989. (In Russian).

[5] Birger I.A., Shorr B.F., Demianushko I.V. and others. *Thermal strength of machine components*. Moscow, Mashinostroenie, 1975, 455 p. (In Russian).

[6] Putchkov I.V. Temis Y.M. Analytical description of the cyclic elastoplastic deformation of structural materials. *J. Strength of Materials*, Vol. 20, Issue 9, pp 1151 – 1156, 1988. (In Russian)

[7] Putchkov I.V. Temis Y.M. Dowson A.L. Damri D. Development of a finite element based strain accumulation model for the prediction of fatigue lives in highly stressed Ti components, *Int. J. Fatigue*, Vol. 17, No. 6, pp 385 – 398, 1995.

[8] Temis Y.M., Azmetov Kh.Kh., Fakeev A.I. LCF simulation under nonisothermal loading. *Mechanical fatigue of metals. Proceeding of 16th international colloquium*, Brno, Czech Republic, pp 208-215, 2012.

[9] Liang Jin, Pelloux R.M., Xie Xishan. Thermomechanical fatigue behavior of a nickel base superalloy, *Chin. J. Met. Sci. Technol.*, Vol. 5, pp 1-7, 1989.

[10] Xijia Wu. Life prediction of Gas Turbine Materials. *Gas turbines*, pp 215-282, 2000.

[11] Temis Y.M., Azmetov Kh.Kh., Zuzina V.M. Low-cycle fatigue simulation and life-time prediction of high stressed structures. *Solid State Phenomena.* Trans Tech Publications, Switzerland, Vols. 147-149, pp 333-338, 2009.

[12] Birger I.A., Dulnev R.A., Balashov B.F. and others. *Structural strength of materials and components of GTE.* Moscow, Mashinostroenie, 1981, 232 p. (In Russian).

[13] Makhutov N.A., Rachuk V.S., Gadenin M.M. *Strength and resource of Liquid-fuel engines.* Moscow, Nauka, 2011, 525 p. (In Russian).

[14] Temis J.M. Applied problems of thermoplasticity analysis. *Engineering Encyclopedia*. Edit. Comm.: K.V. Frolov (Chief) and others. *Dynamics and strength of machines. Mechanism and Machine Theory*. Vol. 1-3 in 2 books. Book 1. Ed. in Chief K.S. Kolesnikov, Moscow: Mashinostroenie, 1994, pp 231-236. (In Russian).

Contact Author Email Address

tejoum@ciam.ru

Copyright Statement